

Washington University in St. Louis  
School of Engineering and Applied Science  
Electrical and Systems Engineering Department

**ESE498**

# **Digital Active Noise Cancelling Headphones**

By

**Michael Jezierny  
Brenton Keller  
Kyung Yul Lee**

Supervisor

**Prof. Robert Morley**

*Submitted in Partial Fulfillment of the Requirement for the BSEE Degree,  
Electrical and Systems Engineering Department, School of Engineering and  
Applied Science,  
Washington University in St. Louis*

**May 2010**

# Table of Contents

Student Statement, Project Abstract, Acknowledgement...4

Problem Formulation...4

Project Specifications...5

Concept synthesis

*Literature Review...*5-7

*Concept Generation and Reduction...*8

Detailed Engineering Analysis and Design Presentation...9-22

Cost Analysis...23

Hazards and Failure Analysis...23

Conclusions...23

References...24-25

# List of Figures and Tables

Figure 1: High-level block diagram of the LMS algorithm.....	6
Figure 2: Noise cancellation by Sony headphones.....	7
Figure 3: Noise cancellation by Bose headphones.....	7
Figure 4: Graphs showing effect step size has on LMS algorithm.....	9
Figure 5: Block diagram of noise cancelling headphones.....	10
Figure 6: LabVIEW VI of NLMS algorithm.....	11
Figure 7: Output of unknown and matching filter as a function of time.....	12
Figure 8: Impulse response of unknown (actual) and matching filter.....	13
Figure 9: RMS noise reduction in dB as a function of time.....	14
Figure 10: of the noise reduction as a function of the number of taps.....	14
Figure 11: Scope capture of the output of the real-time processor on the sbRIO-9631.....	16
Figure 12: Stage 1 of FPGA implementation of NLMS algorithm.....	17
Figure 13: Stage 2 of FPGA implementation of the NLMS algorithm.....	17
Figure 14: Stage 3 of FPGA implementation of the NLMS algorithm.....	18
Figure 15: Block diagram of FPGA simulation VI.....	18
Figure 16: Error between the matching filter and the unknown filter as a function of time.....	19
Figure 17: Amplification and DC bias removal of EA-1843 microphone output.....	20
Figure 18: Frequency plot of outside microphone and output of real-time system without filtering.....	20
Figure 19: Frequency plot of outside microphone and output of real-time system with filtering.....	21
Figure 20: Output of real time system with 150 Hz noise.....	22
Figure 21: Frequency plot of the output of the real-time system.....	22

## **Student Statement**

We affirm that we have applied ethics to the design process and in the selection of the final proposed design.

## **Project Abstract**

In this project, we tried to build noise-cancelling headphones using a two microphone system, one microphone to sample the ambient noise and another to detect how well the noise cancelation is working. We used a finite impulse response (FIR) matching filter to model a system with an unknown transfer characteristic. Then, the output of the matching filter is inverted to create the anti-noise, which is combined electrically with the music and played into the headphones. We simulated our project LabVIEW 8.6 and used LabVIEW Robotics 2009 to implement a real-time system.

## **Acknowledgement**

We would like to thank both Prof. Morley and Ed Richter to help us finish this senior project.

## **Problem Formulation**

We all have trouble listening to music when we are surrounded by noise. For example, it is very difficult to listen to music on an airplane because of its engine noise. However, we all want to enjoy our music whenever, wherever. This motivated us to make noise-cancelling headphones that reduce unwanted ambient sounds.

In order to design the noise-cancelling headphones, we first had to do some research on it. We tried to find articles and patents about the noise-cancelling headphones. After we had done some research, we had to decide how we were going to set up so that we can simulate our algorithm and matching filters. We agreed on using a programming language called LabVIEW. In LabVIEW, we tried to simulate the finite impulse response (FIR) matching filter by using both the least-mean-squares (LMS) and the normalized-least-mean-squares (NLMS) algorithm. Then, we kept designing to try and make it work in real time to solve our problem.

## **Project Specifications**

Our goal in this project was to find a noise-cancellation algorithm and to implement it in hardware; that is, on a pair of non-noise-cancelling headphones. Due to the nature of the project, we did not designate a target level of noise reduction for our algorithm. Instead, our goal was simply to maximize the performance of our algorithm, subject to the constraint that it be readily implementable in hardware. In order to quantify the performance of our algorithm, we have chosen to use a simple measurement. We will test our headphones' ability to provide silence; that is, we will monitor the sound pressure both inside and immediately outside the headphones, while we play a segment of low-frequency noise. Our metric for success will be the root-mean-square noise reduction in decibels; that is,

$$20 \log \left| \frac{\sqrt{\int_t^{t+\tau} V_{\text{inside}}^2(t)}}{\sqrt{\int_t^{t+\tau} V_{\text{outside}}^2(t)}} \right|$$

for some window length  $\tau$ . We wish for this quantity, the RMS noise reduction, to be as high as possible. A high value of the noise reduction will mean that our system is removing most of the incoming noise from the listener's ear.

The final algorithm will be implemented on a National Instruments sbRIO signal processing board, using code created in the LabVIEW program.

## **Concept Synthesis**

### ***Literature Review***

We examined several signal-processing papers while researching the industry standard techniques for active noise cancellation. The unambiguous standard family of algorithms for active noise cancellation is the least-mean-squares (LMS) algorithm and its several descendants. The LMS algorithm and its relatives are all adaptive filtering algorithms. The standard approach to active noise cancellation is to model the transfer function between the ambient noise and the inside of the headphones as some unknown system  $H(z)$ <sup>1</sup>, which we approximate with an adaptive FIR filter having transfer function  $\hat{H}(z)$  and  $p$  coefficients or "taps".

The LMS algorithm [1] uses the following notation

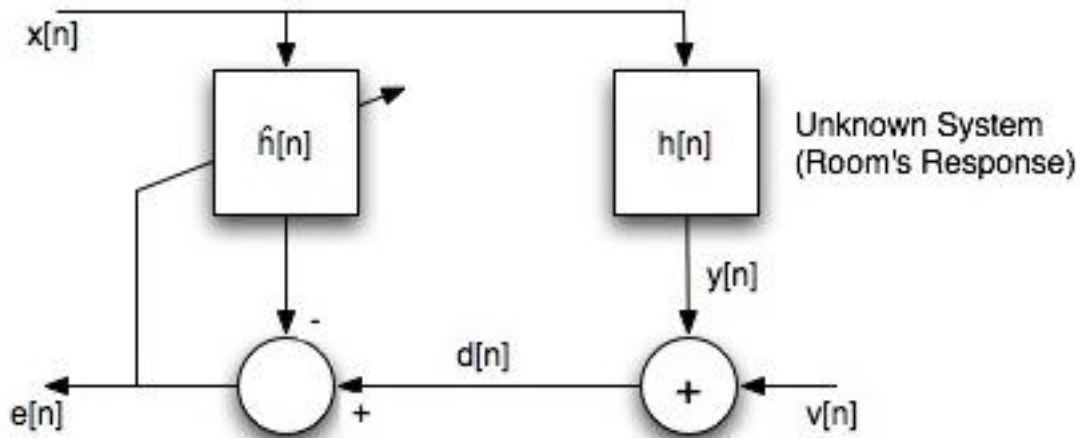
- $x[n]$  is the input to the system

---

<sup>1</sup> We use the transfer function  $H(z)$  and the impulse response  $h[n]$  because we are modeling our system in the discrete-time domain.

- $y[n]$  is the output of the unknown system  $H(z)$
- $\hat{y}[n]$  is the output of the adaptive filter  $\hat{H}(z)$
- $\mathbf{x}[n]$  is a vector of the last  $p$  values of  $x[n]$
- $\hat{\mathbf{h}}[n]$  is the vector of FIR coefficients for  $\hat{H}(z)$ , at the  $n$ th simulation step
- $v[n]$  is the interference
- $d[n] = y[n] + v[n]$
- $e[n] = d[n] - \hat{y}[n]$
- $\mu$  is the “step size” or “learning rate”

We assume that we can only directly measure the quantities  $x[n]$  and  $e[n]$  (we also initialize [to zero], store, and update  $\mathbf{x}[n]$  and  $\hat{\mathbf{h}}[n]$



ourselves).

**Figure 1: High-level block diagram of the LMS algorithm**

See figure 1. The literature [2] shows that the update function that minimizes the mean squared error (hence, “least mean squares”) is

$$\hat{\mathbf{h}}[n + 1] = \hat{\mathbf{h}}[n] + \mu e[n] \mathbf{x}[n]$$

However, some problems are apparent here. The update rate  $\mu$  is chosen arbitrarily. If  $\mu$  is too high, the algorithm will fail to find a local minimum of  $e[n]$  and it will not converge. However, if  $\mu$  is too low, the algorithm will converge very slowly, which would be ineffective.

The normalized LMS (NLMS) algorithm remedies this problem. The NLMS algorithm normalizes the adjustment with the following.

$$\hat{\mathbf{h}}[n + 1] = \hat{\mathbf{h}}[n] + \frac{\mu e[n] \mathbf{x}[n]}{\mathbf{x}[n] \cdot \mathbf{x}[n]}$$

The literature [3] proves that, when the interference  $v[n] = 0$ , the optimal learning rate for the NLMS algorithm is  $\mu = 1$ .

The literature revealed some more exotic methods. For example, some complex noise-cancellation algorithms use only one sensor, but can still approximate the noise [3]. Other researchers suggested variations on the popular LMS algorithm, such as a frequency-divided sub-band FXLMS/FXNLMS algorithm [3], and the MMLMS algorithm which includes delay compensation and back-propagation learning techniques borrowed from artificial neural networks [10].

We also evaluated two commercially available noise-cancelling headsets to measure their performance by our metric. Our results are below. As is clear, the Sony headphones had an average noise cancellation of  $-4.799$  dB, and the Bose headphones had an average noise cancellation of  $-8.734$  dB. We hope to match the performance of these two headphones.

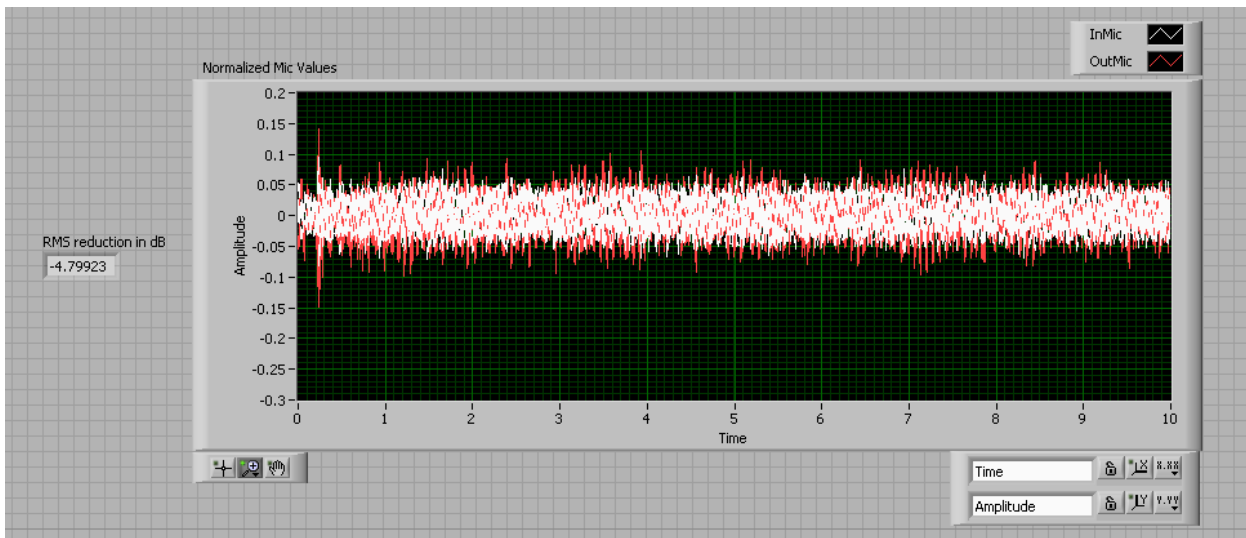


**Figure 2: Noise cancellation by Sony headphones**

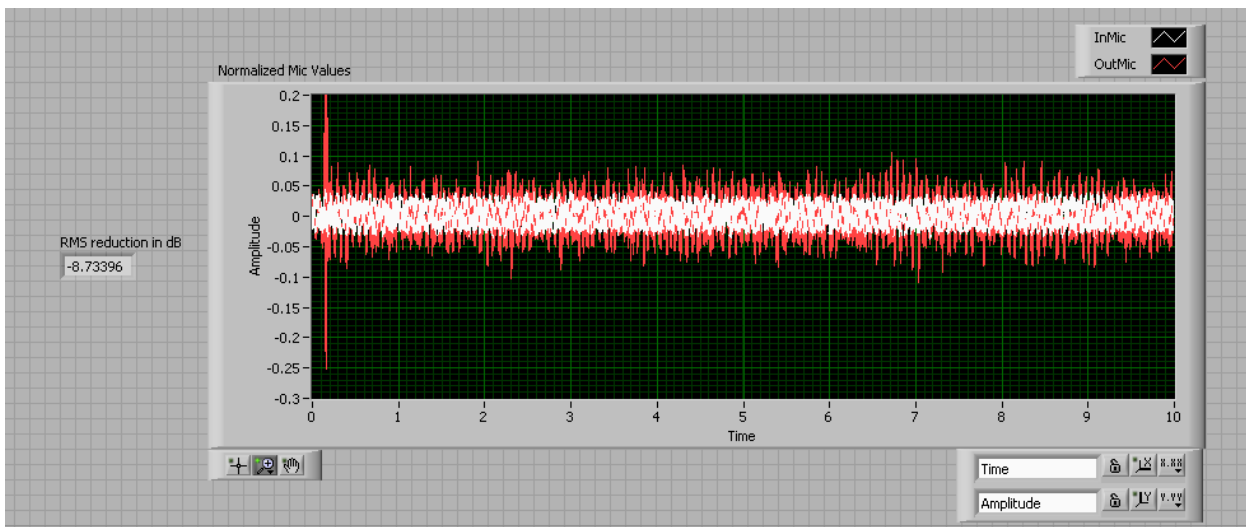


**Figure 2: Noise cancellation by Bose headphones**

### ***Concept Generation and Reduction***

We were faced with choosing between several different varieties of the LMS algorithm, each with its own traits. We first looked at the basic LMS algorithm on which all of the others are based. However, the LMS algorithm has serious problems with its nondeterministic learning rate  $\mu$ . We felt that trying to dynamically change  $\mu$  would be very difficult on an embedded device, like we were targeting. In addition, the performance of the LMS algorithm depends heavily on the scaling of the input  $x[n]$ . In practice, this means that the algorithm may not perform as well on loud noise as on soft noise, to a degree greater than the simple difference in volumes. Most important, however, was the learning rate. Any fixed estimate of  $\mu$  that is conservative enough to guarantee convergence in most cases would take too long to converge in most cases.

We then considered the NLMS algorithm. It is a logical progression from the LMS algorithm, and is not conceptually much more complex than LMS. It is for this reason that we chose NLMS as the primary focus of our design work. However, we did include LMS with a low step size in our early simulation work, as a check that we were implementing everything correctly.

The more complex variations on the LMS algorithm [3] [10] seemed unnecessarily complex. In particular, experimental data did not seem to justify the extra complexity and expense in implementation, especially in the low-power embedded system we had decided to ultimately target. We decided to demote exploration of these algorithms to secondary concern, and ultimately we were not able to deal with them.

A similar concern motivated us to use the feed-forward NLMS algorithm (in which we have both a reference microphone and an error microphone), and not the feedback algorithm [3] (in which we have only the error microphone). The authors of [3] found that the feedback algorithm reduced computational complexity when they were already using sub-band filtering, a technique we decided to avoid. Therefore, we did not think that we would gain enough noise cancellation from the added complexity of using only one sensor in our system.



## Detailed Engineering Analysis and Design Presentation

The first step in our design process was to model the system we would create. In the modeling process we had two major decisions to make. The first decision was how many microphones we would use in our system. In some commercial noise-cancelling headphones 2 microphones are used [8], while some research has been done where only 1 microphone was used [5]. [5] presents a case for using a two microphone system and shows that with that approach he was able to achieve 3 dB better noise reduction than a system with one microphone. We decided to model our system after [5].

The second major decision we needed to make was which algorithm to use to cancel noise. [1] presents two main algorithms for active noise cancellation, least mean squares (LMS) and normalized least mean squares (NLMS), which are described in detail earlier in this document. We decided to use the NLMS algorithm for our implementation. It is computationally more intensive than the LMS algorithm, but the LMS algorithm is not guaranteed to converge. The possibility of the algorithm converging and the rate at which it may converge is heavily dependent on the step size. This principle is illustrated in Figure 4.

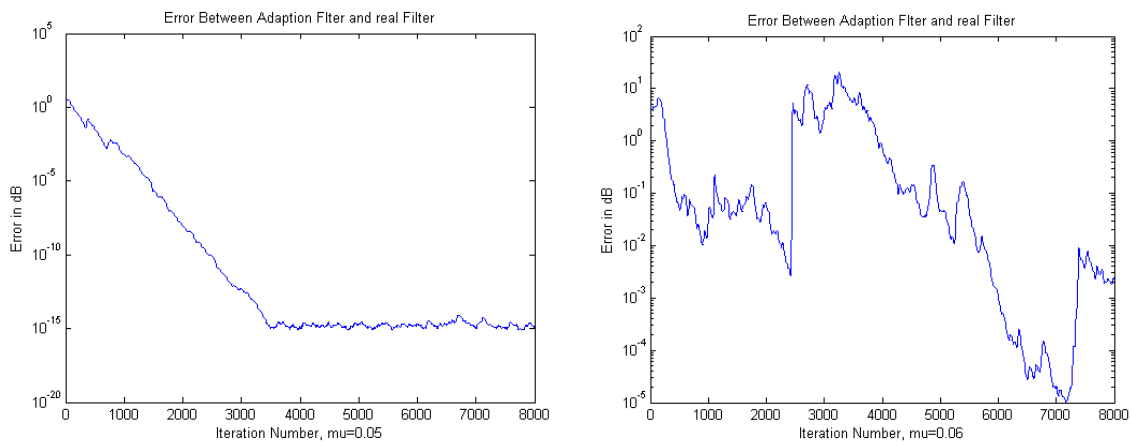


**Figure 4: Graphs showing effect step size has on LMS algorithm. The graph on the left converges, while the graph on the right never does. The difference is step size is .01. Graphs are from [1].**

For the NLMS algorithm it can be shown that a step size of 1 is optimal [9]. With the NLMS algorithm we were able to set a step size one time and were guaranteed that the algorithm would converge.

Once we decided on the number of microphones to use and which algorithm to use, we were able to create a block diagram of our system. Our system consists of two microphones, one outside the headphones and one inside the headphones. The outside microphone detects the noise that is coming into the headphones and is the  $x[n]$  input to the NLMS algorithm. The inside microphone detects how well the noise is being canceled and is the error,  $e[n]$ , input into the NLMS algorithm. The output of the NLMS algorithm is the anti-noise and is played through the headphones. A block diagram is pictured below in Figure 5.

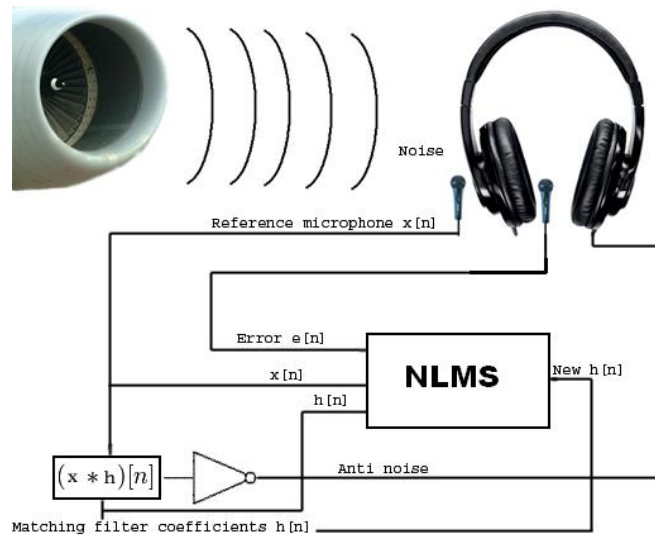


**Figure 5: Block diagram of noise cancelling headphones.**

After setting up a model for our design we began to simulate the model. For our initial simulations we used LabVIEW 8.6. Our first simulation involved implementing the NLMS algorithm in LabVIEW. We created a VI that had an input signal that went into a for-loop. Each iteration of the for-loop was equivalent to one iteration of the NLMS algorithm. A sample from the signal was put into an array at position 0 and this array was our  $x[n]$ . This sample was also put into two different point-by-point FIR sub-VIs, one VI simulated our matching filter and the other VI simulated the unknown filter. The other input to the point-by-point FIR sub-VI was an array of filter coefficients. Our filter coefficients initially were set to zero and were updated each iteration. The filter coefficients for the unknown filter were generated by Ed Richter's LowPassFIRDesign VI. A low-pass filter was used because headphones with passive noise cancellation act as low-pass filters and filter out higher frequency noises. The output of each of the filters was subtracted to find the error term, which was then multiplied by the step size of one. The result was multiplied by the  $x$  vector, divided by the dot product of the  $x$  vector, and added to the old coefficients of the matching filter. In our implementation of the algorithm we had to make one slight modification to avoid an error where the output of our simulation was undefined the first time the VI ran. Initially the  $x$  vector had no elements in it, so each position in the array was set to zero. This

caused a divided by zero error when  $e[n] * x[n] * \mu$  was divided by the dot product of  $x$ . When this happened the output of our matching filter was always not a number (NaN) for the first execution of the VI after it compiled. To fix this problem we set all of the positions in the  $x$  array to  $1 * 10^{-6}$ . This fixed the divide by zero error and also did not impact the performance of the algorithm. The LabVIEW VI for the NLMS algorithm is pictured below in Figure 6.

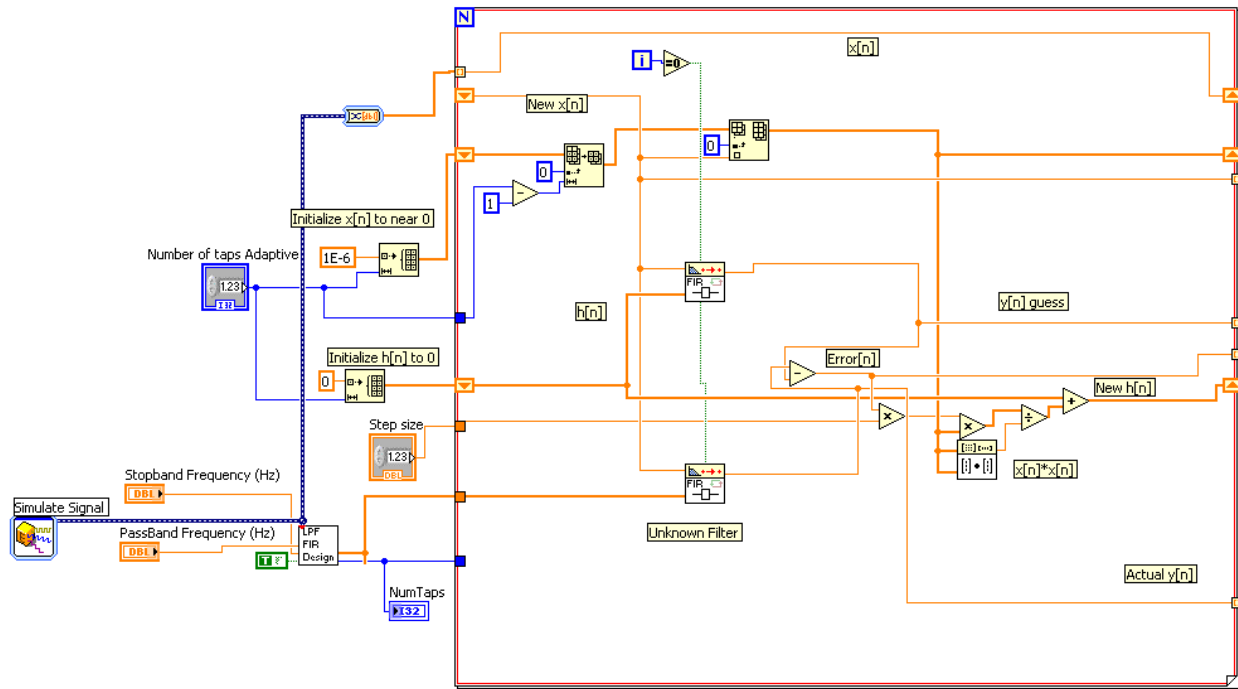


**Figure 6: LabVIEW VI of NLMS algorithm**

The front panel of our VI had three graphs. The first graph displayed the output of the unknown filter and the output of the matching filter as a function of time. The second graph displayed the absolute error between the two filters, and the third graph displayed the impulse response of the two filters. The front panel also had a control for the number of taps for the matching filter and controls for the pass and stop bands of the low-pass filter, which affect the number of taps for the unknown filter. The graphs were how we verified that our implementation was working correctly. Figure 7 shows the output of the unknown filter and the matching filter as a function of time. As the graph shows, our matching filter was able to quickly match the output of the unknown filter. However, in the real system inputs would not be constrained to pure tone sine waves. For our next series of simulations we used actual sound files as the input to our system.

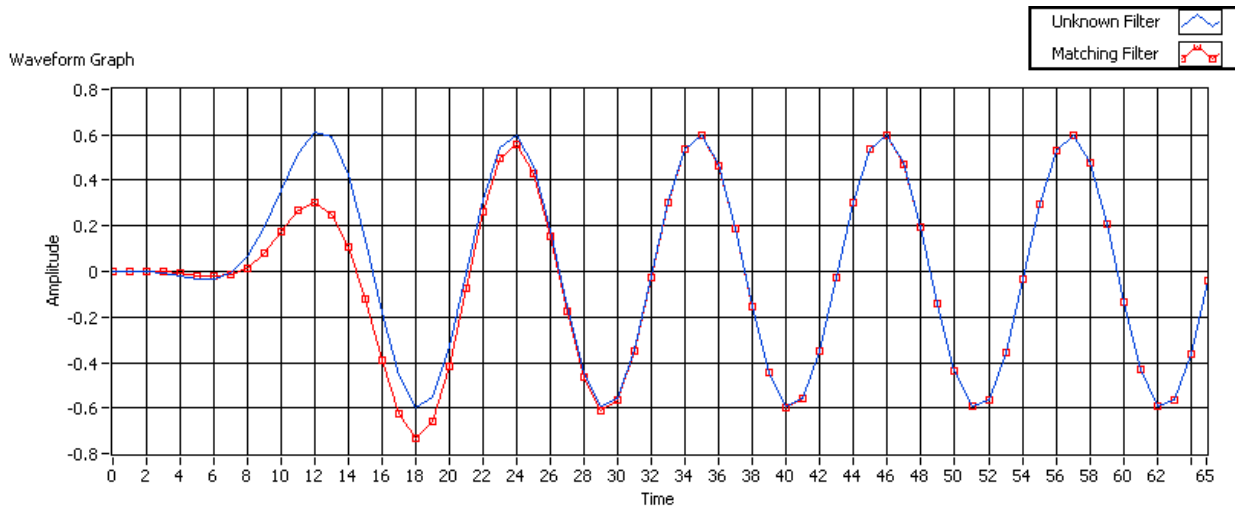


**Figure 7: Output of unknown and matching filter as a function of time. Input signal was a 1 kHz sine wave with amplitude of 1. The unknown filter had the stopband frequency set at 2 kHz, which caused the attenuation.**

The sound file that we used for the next simulation was a car engine noise. We chose a car engine because the noise was repetitive and lower frequency, which are attributes of noise that commercial noise cancelling headphones are good at cancelling as we found. Later we found out that the commercial noise cancelling headphones we had did not cancel this noise well. Eventually we found a different noise file that was more easily cancelled by the headphones we had, but the simulations with the car engine noise were a good place to start. From these simulations we were able to answer an important question about the delays of the filters. Each FIR filter has a delay associated with it that is equal to  $(N-1)/2$ , where  $N$  is the number of taps in the filter. We thought that because the number of taps was different for each filter that the delay for the filters would be different and we would need to compensate for this difference in delay somehow. It turned out that even though the filters had a different number of taps, the delays through the filters were the exact same. This can be explained by looking at the impulse response of the two filters. When the matching filter had more taps than the unknown filter, the algorithm set the taps of the matching filter that would not be in the unknown filter to zero. For example, if the unknown filter had 27 taps and the matching filter had 51 taps, taps, or coefficients, 28-51 were set to zero. Coefficients with a value of zero in the filter do not have an impact on delay, so with the extra taps on the matching filter set to zero, the delays through the filters were the same. Figure 8 shows the impulse response of the two filters after the algorithm has run for the case where the matching filter has more taps than the unknown filter.

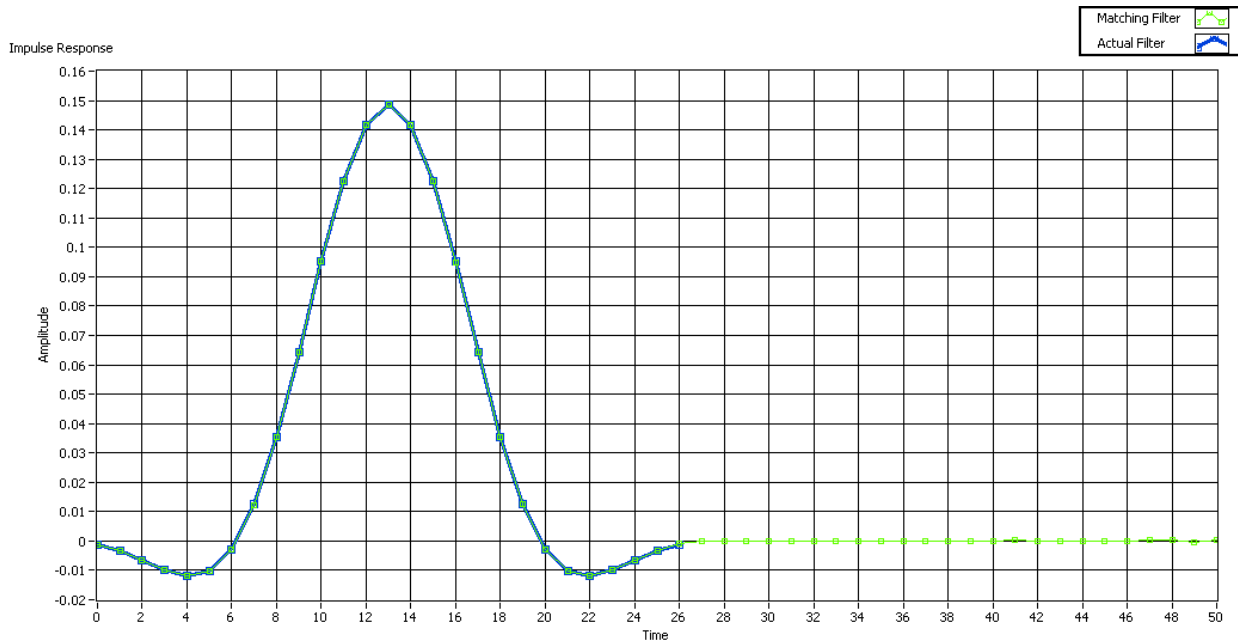


**Figure 8: Impulse response of unknown (actual) and matching filter.**

The graph of the impulse responses of the two filters and the graph of the output of the filters told us that the algorithm was working correctly, but in order to tell how well or system would cancel noise we had to come up with a metric for performance. In commercial headphones and in the research papers we read the standard metric for performance was noise attenuation in decibels (dB) [5][7]. To calculate the noise attenuation in dB we used the error between the two filters and the output of the unknown filter. These values were in arrays in LabVIEW and rather than doing a point by point dB reduction calculation we took the root mean square (RMS) of the arrays and used that to find the noise reduction in dB. We used the RMS value of the arrays because that is how we tested the commercial headphones. The equation to calculate the noise reduction in dB is  $20\log \frac{|e_{RMS}|}{|y_{RMS}|}$  where e is the error array and y is the array of the output of the unknown filter. The output of the RMS noise reduction in dB as a function of time for one of our simulations with the engine noise is pictured below in Figure 9.

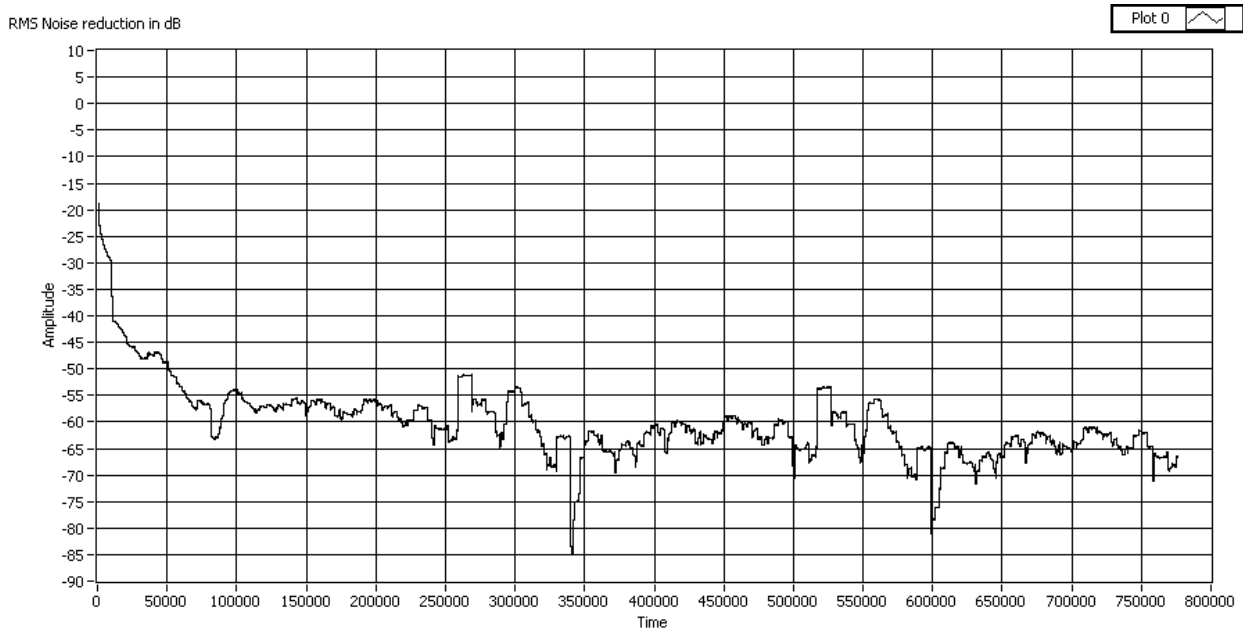


**Figure 9: RMS noise reduction in dB as a function of time**

The amount of dB noise reduction was heavily dependent on the number of taps for the two filters. If the matching filter had less taps than the unknown filter there was very little noise reduction. As the number of taps for the matching filter approached the number of taps for the unknown filter, the noise reduction greatly improved, with the best noise reduction occurring when the two filters had the same number of taps. As the number of taps for the matching filter became greater than the number of taps for the unknown filter the noise reduction decreased, but approached an asymptote. A graph of the noise reduction as a function of the number of taps for the matching filter is pictured below in Figure 10; the unknown filter had 51 taps.

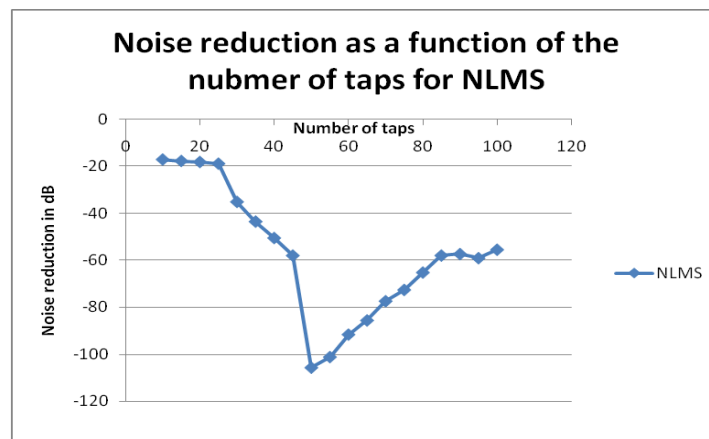


**Figure 10: Graph of the noise reduction as a function of the number of taps.**

In the real-time system we would need to decide how many taps our matching filter would use. Because the noise reduction was heavily dependent on the relative number of taps, we wanted to see if we could find out approximately how many taps there might be in the unknown filter (headphones)

based on the delay from the outside of the headphones to the inside of the headphones. We set up a test to try and see if there was any delay from the time a microphone outside the headphones picked up a signal to the time a microphone inside the headphones picked up a signal. We found out that there was almost no discernable delay with the tools we used, not surprising given the speed of sound, and were not able to get a better idea of how many taps the unknown filter might have.

To demonstrate how our system would ideally work we added in music to our simulation. The music was added to the difference between the matching and unknown filters, played out through the sound card and written to a file. On the front panel we added a switch that gave the option of cancelling the noise.

Our simulations worked well, but our goal was to try and actually implement real-time noise cancelling headphones. In order to accomplish this we needed to change to a real-time platform because the code that we had would not run in real time. Because we had already done all of our simulations in LabVIEW we decided to use the National Instruments sbRIO-9631, which is a real time system that can run using LabVIEW code. Initially we tried to port our code directly over to the sbRIO-9631 to run on its processor, but we found that the processor could not sample the analog to digital converter (ADC) and put it back out to the digital to analog converter (DAC) faster than around 1 kHz without jitter. Jitter would have caused unwanted noise in the output of our algorithm. The sample rate of 1 kHz was without running any code on the processor, so that sample rate would have only gotten worse had we tried to also run the NLSM algorithm. This sample rate was too slow for what we wanted to accomplish. With a sampling rate of 1 kHz (and more than likely much lower) we could have only sampled and cancelled noises from 0-500 Hz. Figure 11 demonstrates the jitter that the real-time processor exhibited.

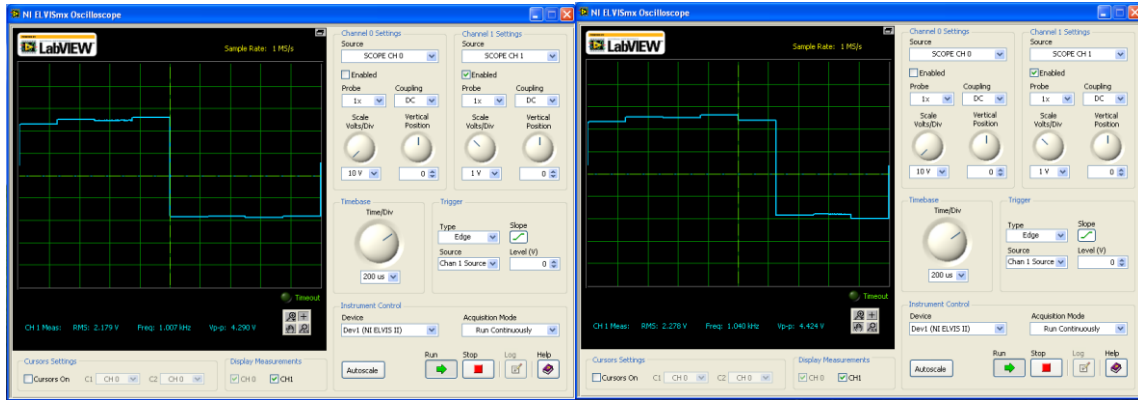


**Figure 11: Scope capture of the output of the real-time processor on the sbRIO-9631. The sample rate was set to 4 kHz and the input was a 500 Hz square wave. The first capture shows a normal output and the second capture shows a missed output.**

The sbRIO-9631 also has an FPGA on board that has access to the ADC, DAC, and can sample at 50 kHz. The FPGA does not have to deal with operating system overhead like the real-time processor and can have code written for it in a modified version of LabVIEW. Because the real-time processor could not run fast enough and because the FPGA had the ability to run the algorithm without jitter, we chose to implement our real-time system on the FPGA on the sbRIO-9631. We were unable to directly port our simulation over to the FPGA because our simulation used some sub-VI's that were unavailable on the FPGA and because our simulation used floating point numbers and operations. LabVIEW code for the FPGA does not work with floating point numbers, so we had to remake our LabVIEW code using only fixed point operations. We simulated the FPGA code in LabVIEW 8.6 instead of LabVIEW 2009 because it is easier to probe and debug in LabVIEW 8.6. We decided to split the algorithm up into four separate stages, using a sequenced structure that would execute one section at a time to conserve and reuse resources, like multipliers and adders, on the FPGA. All calculations, except the divide in stage 3, were done using 16-bit integers. The first stage of the fixed point implementation adds a new element to the x array and convolves x and the coefficients h. The result of the convolution was subtracted from the output of the unknown filter. Stage one is pictured in Figure 12.



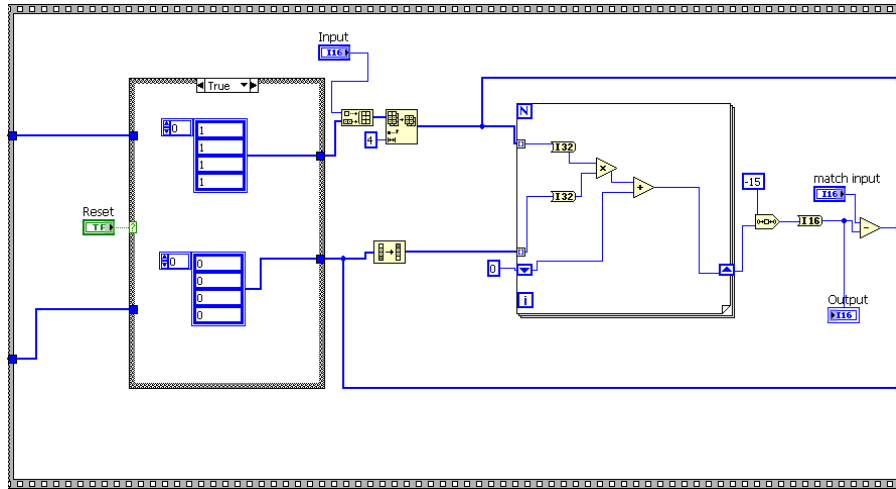


Figure 12: Stage 1 of FPGA implementation of NLMS algorithm.

The second stage computed the dot product of  $x$  with  $x$  and multiplied each value in the  $x$  array by the error and step size. Stage 2 is pictured in Figure 13.

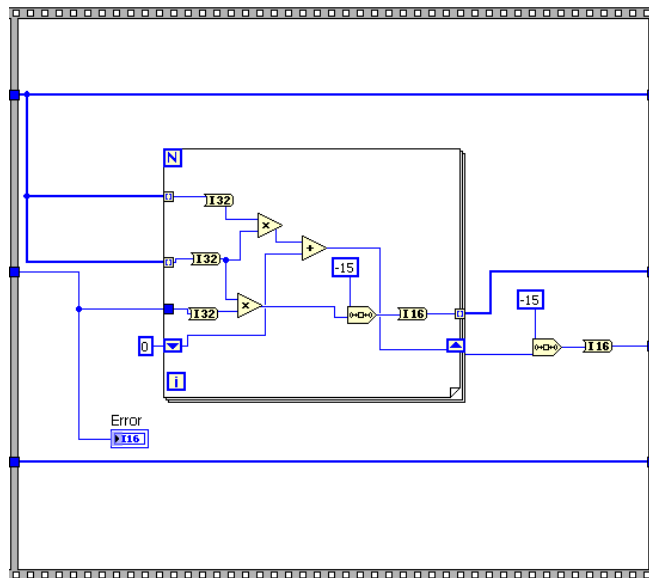
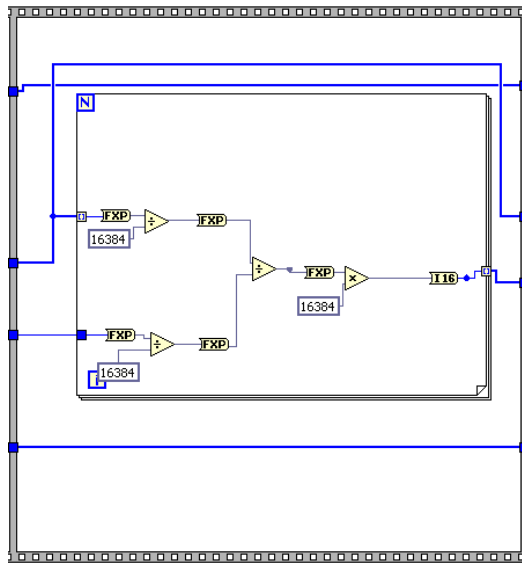


Figure 13: Stage 2 of FPGA implementation of the NLMS algorithm.

Stage 3 was the most difficult stage to code because of the division that was required. In order to do the division the 16-bit integers had to be converted into fixed point numbers. The problem then became where to put the radix point. Initially we represented the fixed point numbers in 1.15, which allowed us to represent the numbers  $-1$  to  $.9999$ . However, when running through the simulations we found that the result of some divisions were greater than 1, which 1.15 cannot represent. To solve this problem we changed to 2.14 representation so we would be able to represent numbers between  $-2$  and  $1.999$ . To convert the 16-bit integers into fixed point notation we converted the integers to fixed point, then divided by  $16384$  ( $2^{14}$ ). Once the numbers were in 2.14 representation we executed the divided for

the NLMS algorithm and cast it into a 2.14 fixed point number. We then multiplied the result by 16384 and cast it back into a 16-bit integer. Stage 3 is pictured below in Figure 14.



**Figure 3: Stage 3 of FPGA implementation of the NLMS algorithm.**

Stage 4 added the result of stage 3 to the old coefficients to get the new set of coefficients.

To simulate the design and verify that it would converge, we set up a test similar to the setup in the first simulation. We had an input signal that went to an unknown FIR and to the NLMS VI. The output of the unknown FIR was the second input to the NLMS VI. The unknown FIR used  $8192 = .5$  for all of its coefficients. We then checked the error between the outputs of the two filters and the outputs themselves. The VI for the FPGA simulation is pictured below in Figure 15.

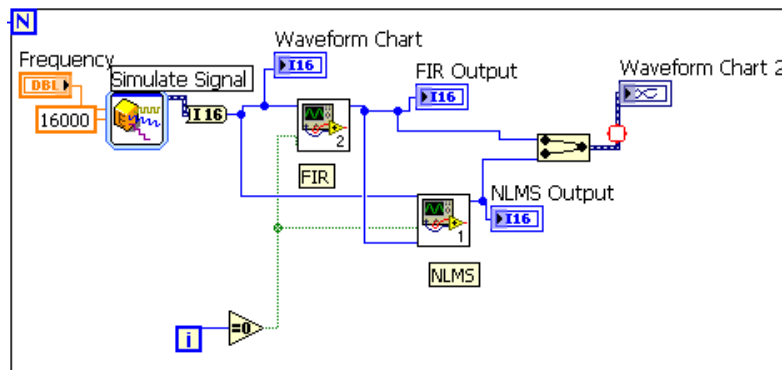


**Figure 15: Block diagram of FPGA simulation VI**

The input signal to both the unknown filter and the NLMS VI was a 100.1 Hz sine wave with amplitude 16000. A full-scale sine wave was not used because of overflow problems with the divide operation. The error output of one simulation is pictured below in Figure 16.

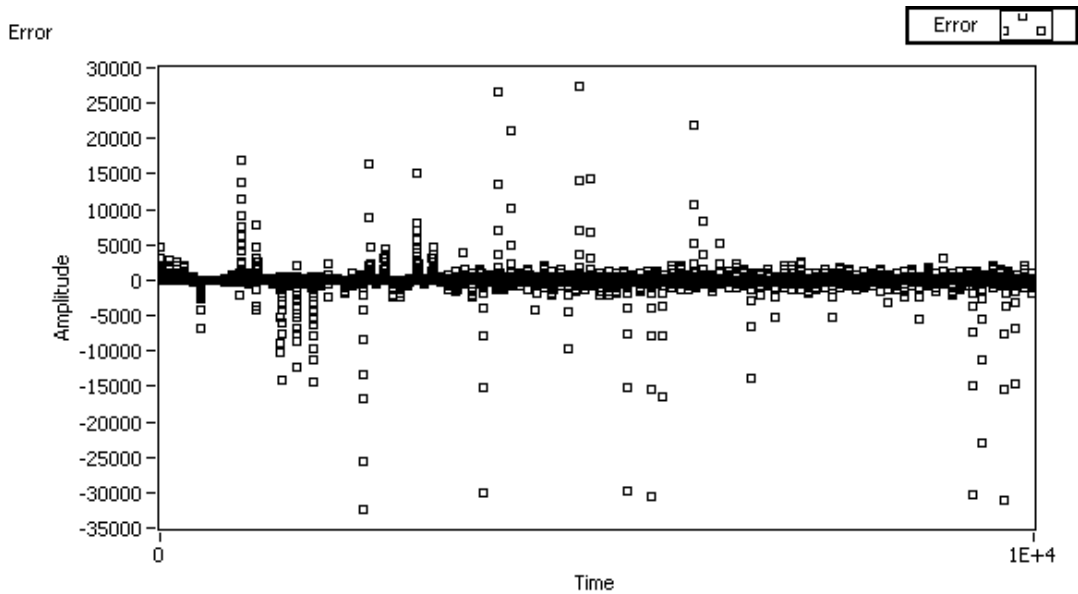


**Figure 16: Error between the matching filter and the unknown filter as a function of time for FPGA simulation.**

This simulation shows the algorithm converges and does work using only integers and fixed point numbers. We then implemented the exact same NLMS, FIR and test VIs in LabVIEW 2009 for an FPGA and simulated them.

After simulation, we compiled our FPGA VI, loaded it onto the sbRIO-9631, and created another VI that ran on the processor for debugging purposes. The front panel of the VI that ran on the processor had three graphs; one for each microphone and one for the output of the NLMS algorithm. For the outside microphone we used a dbx RTA-M microphone connected to an ART USB Dual Pre preamplifier. The inside microphone needed to be able to fit inside of an ear, so we used an EA-1843 electret microphone. In order to get the output of the microphones into the sbRIO we had to modify the signals coming out of the microphones. The dbx RTA-M was connected to a preamplifier, which easily allowed us to control the gain on the output of the microphone, but the EA-1843 was not connected to a preamp. We had to amplify the signal coming out of the EA-1843 microphone and also remove a DC offset that the microphone had. To amplify the signal we used a Texas Instruments LF347N op-amp with a gain of around 90x. To remove the DC offset we put the output signal of the amplifier through an AC coupling circuit. We used a 2.2 $\mu$ F capacitor and a 7.5 k $\Omega$  resistor in series with a 470 $\Omega$  resistor to accomplish this. Because of its large capacitance, this circuit also did not attenuate any signals of interest. Figure 17 illustrates the effect the amplification and AC coupling had on the signal from the EA-1843 microphone.

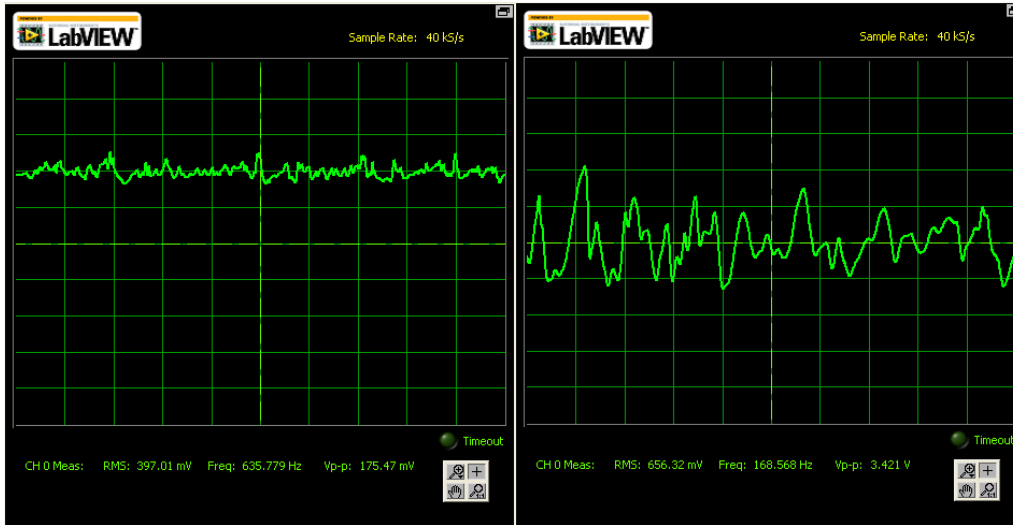


**Figure 17: Amplification and DC bias removal of EA-1843 microphone output. Left - Signal from the output of the EA-1843 microphone. Right - Signal after amplification and removal of DC bias.**

Although the dbx RTA-M microphone had its own preamplifier and was already AC coupled, we still had to modify the signal before we put it into the sbRIO to run the algorithm. The main problem with the dbx microphone was that it picked up frequencies that were not of interest to our noise cancelling algorithm. We were trying to cancel low frequencies, around 1 kHz, and this microphone picked up frequencies in the 6-10 kHz range. These frequencies, when input into our algorithm, caused the output to be a high pitched noise at all times. To solve this problem we put the output of the two channels of the dbx microphone through and the output of the algorithm through a low-pass filter. We used a .01 $\mu$ F capacitor in series with a 12k $\Omega$  resistor as the low-pass filter, which had a cutoff frequency of ~1.3 kHz. These low-pass filters had the desired effect and removed the higher frequencies from our system. Figures 18 and 19 illustrate this point.

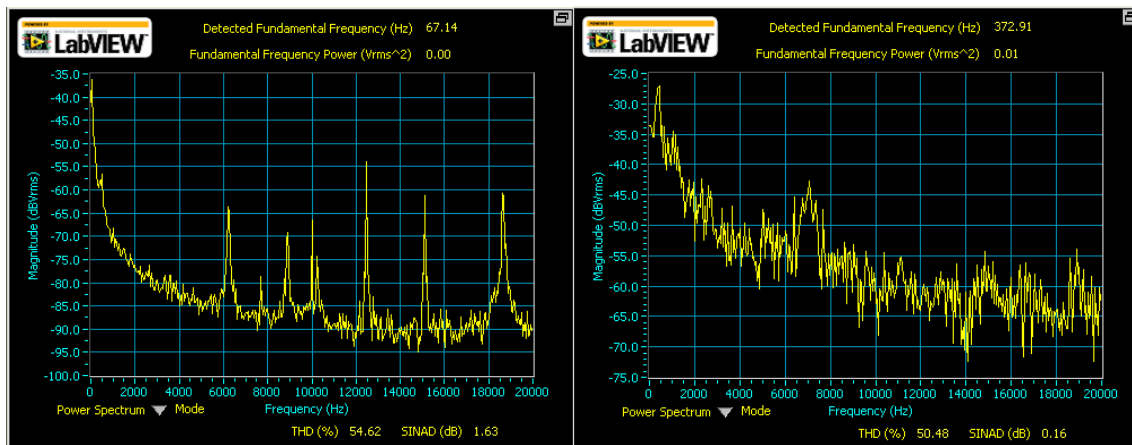


**Figure 18: Left-Frequency plot of the output of the outside microphone with no filter. Right-Frequency plot of the output of the system with no filter on the microphone or the output of the system.**

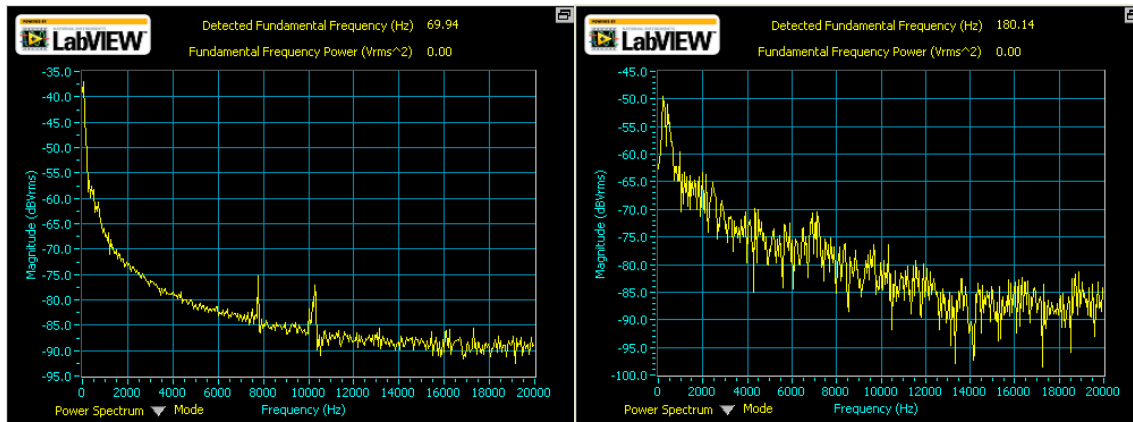


**Figure 19: Left-Frequency plot of the output of the microphone after filtering. Right-Frequency plot of the output of the system with filters on the microphone and on the output of the system.**

After filtering the reference microphone input and filtering the output of the system we were ready to try and listen to the output of our system. The sbRIO-9631 analog output has a voltage range of  $\pm 10$  volts, which is much larger than what headphones take as an input voltage. Headphones take in use voltages around  $\pm 1$  volt, so we put the output through a resistive divider to lower the output voltage of the system down to around  $\pm 1$ . We used a 91 k $\Omega$  and a 910 k $\Omega$  resistor to achieve a .09 gain.

With the output now down in the voltage range that could go into headphones, we tried to take the divided output and put it directly onto the headphones. We found that the divided output was not able to drive the headphones, so to solve this problem we put the output back into LabVIEW, not on the robot, but running on the computer. We put the output into an analog input, and had the VI run in a loop that took the analog input and put it out to the analog output. The loop sampled the input at 50 kHz for .1 seconds and then output it to the analog output. From the analog output we were able to put the output signal onto the headphones. There was however one main problem with this solution. With this solution there was about a half second delay from the output of the sbRIO-9631 system to when it got to the headphones.

To test our system we played a low-frequency noise file that we found online. The frequency of the noise was around 150 Hz. This was the same noise file that we used to test the Bose and Sony commercial headphones. Unfortunately our real-time system was unable to cancel the noise. The outside microphone picked up the noise and the output changed when the noise was introduced, but the noise was not canceled, as noted by no decrease in the output of the error microphone. The output of the system did have power at the correct frequency around 150 Hz though. A screen capture from the test is pictured below in Figure 20. A frequency plot of the output is pictured in Figure 21.

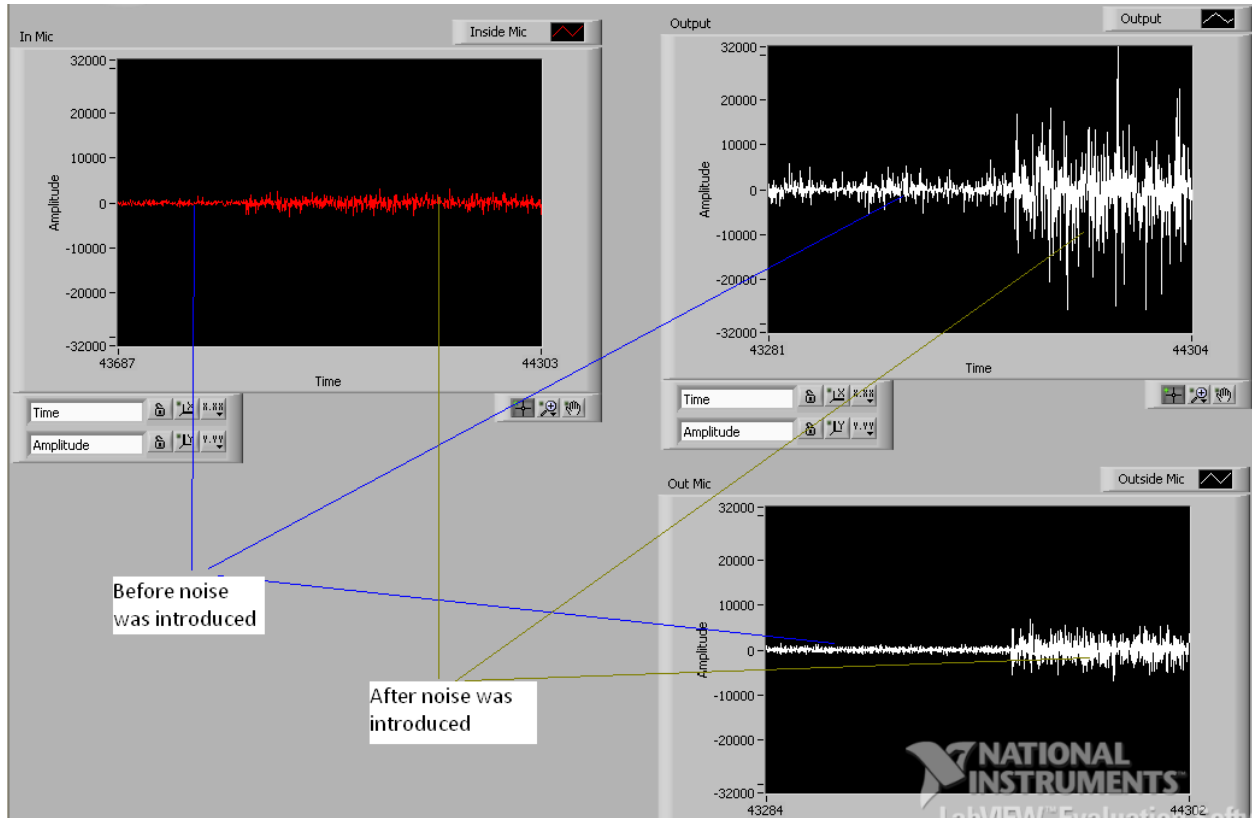


Figure 20: Output of real time system with 150 Hz noise. Top left graph is output from inside microphone, top right is output of the system and bottom right is the output of the outside microphone.

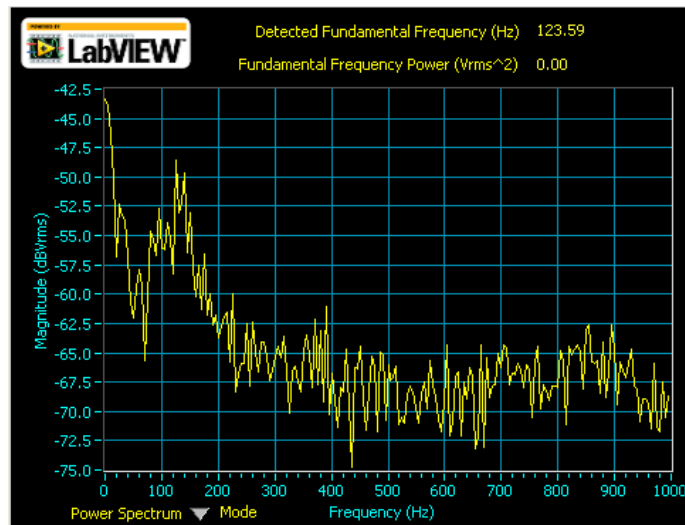


Figure 21: Frequency plot of the output of the real-time system.

## **Cost Analysis**

The most expensive element needed to prototype this design was the sbRIO-9631 and the LabVIEW software. In order to obtain pricing information on the RIO, one must contact National Instruments directly and real-time LabVIEW can be purchased for \$3,077 [11]. We also used the NI ELVIS II board, which can be purchased for \$2,665 [12]. Fortunately as students of Washington University we were able to use these tools for free. The microphones we used were property of the department also, but can be purchased for \$17.25 [13] (for a similar EA microphone) and for \$99 [14]. The preamplifier can be purchased for \$79.97 [15].

## **Hazards and Failure Analysis**

Most of our design was done in simulation, which poses no safety threat. The only threat our real-time system might impose would be damaging the ears of the person wearing the headphones, but we set a limit to the voltage that we allowed to go into the headphones so that it would not be too loud.

## **Conclusions**

We were able to simulate a correctly functioning noise cancelling system in LabVIEW that was able to reduce noise by as much as 81 dB RMS. However, we were unable to transform the simulation into a functioning real-time system. In retrospect, most of our efforts were spent in the simulation aspect of the design process. More time needed to have been spent on developing the real-time system in order to have made it work. In its current state the real-time system shows some promise for eventually working as the output responds differently for different inputs and the output has power at the correct frequency. We think that one of the main reasons for this design's failure has to do with the microphones. Both microphones were unable to be sensitive enough to pick up soft noises, such as a fan in the room or the test file not turned up all the way, without having a lot of noise in the signal as well. We needed both microphones to have a better signal to noise ratio, so that the input to the system from both microphones was as close to the actual outside noise as possible similar to the simulations. The noise on the outside microphone was especially disruptive to the system. If we had to do the project over again, we would be more careful in picking out microphones and try to find noise cancelling microphones to use for both the inside and outside microphones. As we mentioned earlier in the design portion of the paper, the output of our system had to go back into LabVIEW before being output to the headphones. This might have also been a source failure, because of the extra delay that was added to the real-time system. Ideally we would have liked to have had the output of the sbRIO go directly into a pair of headphones.

## **References**

- [1] A. Milosevic and U. Schaufelberger. (2005 December). Active Noise Control. Rapperswil, Switzerland. [Online]. Available: [http://www.medialab.ch/archiv/pdf\\_studien\\_diplomarbeiten/da05/da2005-104\\_ActiveNoiseControl.pdf](http://www.medialab.ch/archiv/pdf_studien_diplomarbeiten/da05/da2005-104_ActiveNoiseControl.pdf)
- [2] B. Brogdon, T. Deitch, K. Barnhart, and B. Antley, (2008, January), "Least mean squares adaptive filters," *Connexions*, Available: <http://cnx.org/content/m15675/1.2/>
- [3] B. Siravana, N. Magotra, and P. Loizou, "A novel approach for single microphone active noise cancellation," presented at 45<sup>th</sup> IEEE MWSCAS Conf., Tulsa, Oklahoma, Aug. 4-7, 2002.
- [4] G. S. Kang and L. J. Fransen, "Experimentation with an adaptive noise-cancellation filter," *IEEE Trans. on Circuits and Systems*, vol. CAS-34, pp. 753-758, Jul. 1987.
- [5] K. C. Zangi. (1993) A New Two-Sensor Active Noise Cancellation Algorithm. Cambridge, MA. [Online]. Available: <http://www.rle.mit.edu/dspg/documents/Two-sensoractive.pdf>.
- [6] Milosevic and U. Schaufelberger, "Active noise control," Diploma thesis, University of Applied Sciences Rapperswil, Rapperswil, Switzerland, 2005.
- [7] Noise Cancelling Headphones. Sony Electronics Inc. Tokyo, Japan. [Online]. Available: <http://www.sonystyle.com/webapp/wcs/stores/servlet/ProductDisplay?catalogId=10551&storeId=10151&langId=-1&productId=8198552921665368379>
- [8] QuietComfort® 15 Acoustic Noise Cancelling® headphones. Bose Corporation. The Mountain, Framingham, MA. [Online]. Available: [http://www.bose.com/controller?url=/shop\\_online/headphones/noise\\_cancelling\\_headphones/quietcomfort\\_15/index.jsp](http://www.bose.com/controller?url=/shop_online/headphones/noise_cancelling_headphones/quietcomfort_15/index.jsp)
- [9] Wikipedia Contributors. (2010, April). Least mean squares filter. [Online]. Available: [http://en.wikipedia.org/wiki/Least\\_mean\\_squares\\_filter](http://en.wikipedia.org/wiki/Least_mean_squares_filter)
- [10] Z. Feng, X. Shi, and H. Huang, "An improved adaptive noise cancelling method," *Canadian Conference on Electrical and Computer Engineering*, 1993, pp. 47-50.
- [11] National Instruments Corporation. Austin, TX. [Online]. Available: [http://ohm.ni.com/advisors/devsuite?rec=Realtime\\_FPGA](http://ohm.ni.com/advisors/devsuite?rec=Realtime_FPGA)
- [12] National Instruments Corporation. Austin, TX. [Online]. Available: <http://sine.ni.com/nips/cds/view/p/lang/en/nid/13137>
- [13] Digi-Key Corporation. Thief River Falls, MN. [Online]. Available: <http://search.digikey.com/scripts/DkSearch/dksus.dll>
- [14] zZounds Music, LLC. Midland Park, NJ. [Online]. Available: <http://www.zzounds.com/item--DBXRTAM>



[15] Sweetwater Sound Inc. Fort Wayne, IN. [Online]. Available:  
<http://www.sweetwater.com/store/detail/USBDualPrePS>